

## Dynamical origin of deterministic stochastic resonance

Kenichi Arai, Kazuyuki Yoshimura, and Shin Mizutani

*NTT Communication Science Laboratories 2-4, Hikaridai, Seika-cho, Soraku-gun, Kyoto 619-0237, Japan*

(Received 29 March 2001; revised manuscript received 7 September 2001; published 20 December 2001)

We numerically demonstrate stochastic-resonance-like behavior in a deterministic chaotic oscillator system, using a modified Rössler system driven by a sinusoidal external force: intermittent  $2\pi$  phase slips between the system and the external force synchronize with a periodic input signal that weakly modulates the external force in an appropriate parameter range. We show that the dynamical mechanism of this stochastic-resonance-like behavior is explained by a boundary crisis that depends on two bifurcation parameters.

DOI: 10.1103/PhysRevE.65.015202

PACS number(s): 05.45.Xt, 02.50.Ey

During the last decade, stochastic resonance (SR) has been extensively studied in a number of electrical, optical, and neuronal systems (see Ref. [1] and references therein). To date, most studies on SR have been carried out for systems with stochastic noise. However, it is natural to look for SR-like phenomena in deterministic chaotic systems since chaotic fluctuation is similar to noise. Anishchenko *et al.* numerically demonstrated in Ref. [2] that an SR-like phenomenon can be caused by internal chaotic dynamics rather than stochastic noise. They used the dynamics of a one-dimensional chaotic map in the vicinity of a band-merging crisis and showed that the intermittent hopping between two different chaotic repellers synchronizes with the external periodic signal. The SR-like phenomenon in chaotic systems without stochastic noise is called *deterministic stochastic resonance* (DSR). DSR has been reported for certain other chaotic systems: numerically for the forced double-well Duffing system [3] and also in ferromagnetic resonance [4] and chaotic CO<sub>2</sub> laser [5] experiments. However, the dynamical mechanism of DSR has yet to be fully understood, in that no one has provided a theoretical explanation of DSR in terms of the dynamics: it has not been clarified what type of crisis leads to DSR and how the crisis depends on the bifurcation parameters is essential for DSR although some relationship between a crisis and DSR has been pointed out based on numerical experiments [2].

In this paper, we demonstrate that a chaotic oscillator system with a weak periodic input signal exhibits DSR. We then show theoretically that DSR in that system is caused by a boundary crisis that induces a collision between an attractor and a periodic orbit on its basin boundary. We specially emphasize that the DSR mechanism is explained using the scaling law of two bifurcation parameters in the boundary crisis.

We employ a modified Rössler system driven by a sinusoidal external force [6], where the coupling strength of the external force is weakly modulated by a periodic modulating signal,

$$\begin{aligned}\dot{x} &= s(-\nu y - z), \\ \dot{y} &= s(\nu x + ay) + K[1 + \epsilon \sin(\omega t)]\sin(\Omega t), \\ \dot{z} &= s[b + z(x - c)],\end{aligned}\quad (1)$$

where  $\nu$ ,  $a$ ,  $b$ ,  $c$ ,  $K$ ,  $\epsilon$ ,  $\omega$ , and  $\Omega$  are constants. Throughout this paper, we set  $a=0.20$ ,  $b=0.20$ ,  $c=4.80$ ,  $\omega=6.0$

$\times 10^{-4}$ , and  $\Omega=1.077$ . We introduce the cylindrical coordinate  $(\theta, r, z)$  defined by  $x=r\cos\theta$ ,  $y=r\sin\theta$ , and  $z=z$ . In Eq. (1),  $s=1+\alpha(r^2-\bar{r}^2)$ , where  $\bar{r}$  is the average value of  $r$  for an ordinary Rössler oscillator ( $\alpha=K=0, \nu=1$ ) and we set  $\alpha=2.0\times 10^{-3}$ . The projection of the attractor on the  $x$ - $y$  plane forms a ring, in which a phase point always rotates around the origin. Therefore, we can use  $\theta$  as the phase of the chaotic rotation. We adopt a  $\theta$  value that is continuous with respect to time: i.e., we distinguish integer multiples of  $2\pi$  differences of  $\theta$ .

First, we consider the case of  $\epsilon=0$ . We focus on the phase difference  $\Delta\theta=\theta-\Omega t$ . If  $K$  is larger than a critical value  $K_c$ ,  $\Delta\theta$  is confined within a small range for *all time* while the amplitude  $r$  still fluctuates chaotically. This phenomenon is called chaotic phase synchronization [6,7]. In contrast, for  $K<K_c$ ,  $\Delta\theta$  increases in time with intermittent  $2\pi$  jumps although  $\Delta\theta$  is almost constant except for these jumps.

Figure 1 shows the time evolution of  $\Delta\theta$  for certain values of  $\nu$ . The phase difference  $\Delta\theta$  increases with a sequence of  $2\pi$  jumps. These jumps are called phase slips and occur more frequently as  $\nu$  increases. Therefore,  $\nu$  can be regarded, in a sense, as a parameter for controlling the intensity of internal chaotic fluctuation. We use  $\nu$  as a control parameter that allows us to observe DSR.

We then consider a system whose coupling strength is modulated by a weak signal, that is,  $\epsilon\neq 0$ . Figure 2 shows that this modulation drastically changes the probability distribution  $\rho(\tau)$  of interslip intervals, which are durations be-

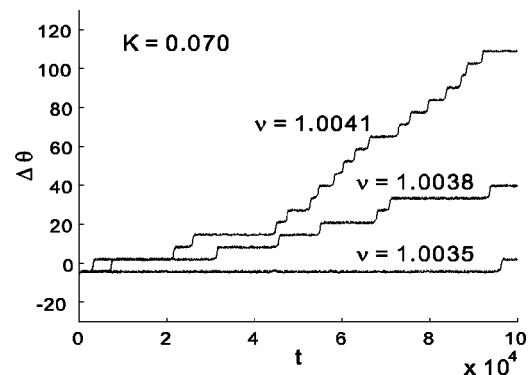


FIG. 1. Time evolution of phase difference  $\Delta\theta$ .

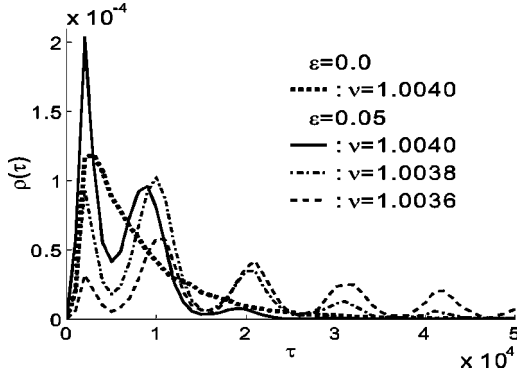


FIG. 2. Inter-slip interval distribution  $\rho(\tau)$  without a modulating signal ( $\epsilon=0$ ) and with a signal ( $\epsilon=0.05$ ).

tween two consecutive slips. Without the signal, the distribution is unimodal and decays exponentially for large  $\tau$ , but with the signal, it develops multi-peaks. The peaks are centered at integer multiples of the period  $2\pi/\omega$  of the modulating signal. This implies that phase slips are most likely to occur for a certain phase of the modulating signal. We can also say that the phase slips synchronize statistically with the signal.

In Fig. 3, the difference  $\Delta\rho_n = \rho_{\epsilon=0.05}(\tau_n) - \rho_{\epsilon=0}(\tau_n)$  in the  $n$ th peak height with and without the modulating signal is plotted versus  $\nu$  for  $n=1,2$ , where  $\rho_{\epsilon=0.05}$  and  $\rho_{\epsilon=0}$  represent  $\rho(\tau)$  for  $\epsilon=0.05$  and  $\epsilon=0$ , respectively, and  $\tau_n = 2\pi n/\omega$ . The difference  $\Delta\rho_1$  for the first peak has a maximum value at  $\nu \approx 1.0038$ . For the second peak,  $\Delta\rho_2$  has its maximum at  $\nu \approx 1.0036$ , which is smaller than  $\nu$  for  $\Delta\rho_1$ . Coherent behavior with the signal appears for an appropriate value of  $\nu$ , that is, for an appropriate intensity of internal randomness. It should be emphasized that this resonant behavior in  $\Delta\rho_n$  coincides with the characteristics of SR. This SR-like behavior is caused not by external stochastic noise but by chaotic internal fluctuation. Therefore, we call this DSR.

Below, we clarify the dynamical mechanism of DSR. We start with an approximate theory, which is based on a Poisson process approximation [8,9]. Figure 2 indicates that for  $\epsilon=0$ ,  $\rho(\tau)$  can be well fitted to the exponential distribution

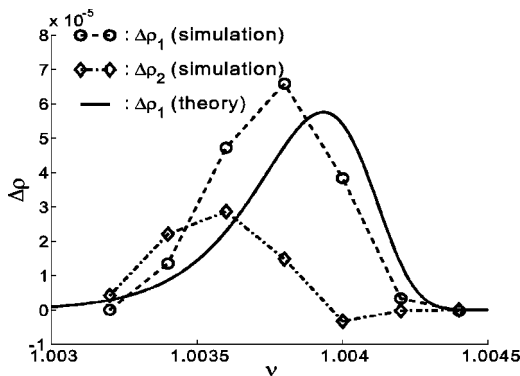


FIG. 3. Difference  $\Delta\rho_n$  between  $\epsilon=0.0$  and  $\epsilon=0.05$  versus  $\nu$ .  $n=1$  ( $\circ$ ) and  $n=2$  ( $\diamond$ ). The theoretical curve is also shown as a thick solid line.

except in a small  $\tau$  range, i.e.,  $\rho(\tau) \approx \lambda \exp(-\lambda\tau)$ , where the constant  $\lambda$  represents the phase slip rate. The deviation from  $\lambda \exp(-\lambda\tau)$  in the small  $\tau$  range means that there is some refractory time in successive phase slips. The exponential form of  $\rho(\tau)$  in the large  $\tau$  range implies that successive phase slips are statistically independent: the probability of a phase slip occurring during a short period  $\Delta t$  is given by  $\lambda\Delta t$ , with no memory. When  $\epsilon=0$  in Eq. (1), the rate  $\lambda$  is a function of  $K$  and  $\nu$ , namely,  $\lambda = f(K, \nu)$ .

For  $\epsilon \neq 0$ ,  $\rho(\tau)$  differs from the exponential distribution. In the present study, we consider the case of a slowly varying periodic signal, i.e.,  $\omega \ll 1$ . This condition means we can assume that the periodic signal only modulates the rate  $\lambda$ , that is, the occurrence of phase slips still follows a Poisson process with the *time-dependent* rate.

Suppose that one phase slip occurs at  $t=t_0$  and that the phase of the modulating signal at time  $t_0$  is  $\phi_0 = \omega t_0 \bmod 2\pi$  ( $0 \leq \phi_0 < 2\pi$ ). We define a new time variable as  $\tau = t - t_0$ . The time-dependent rate is given as a function of  $\tau$  and  $\phi_0$ , and we denote it by  $\lambda(\tau|\phi_0)$ . The probability that the next phase slip occurs at time  $\tau$  can be given by  $P(\tau|\phi_0) = \lambda(\tau|\phi_0) \exp[-\int_0^\tau \lambda(\tau'|\phi_0) d\tau']$ . When the modulating signal is imposed, the time dependence of  $\lambda(\tau|\phi_0)$  arises from the modulation of variable  $K$  in  $f(K, \nu)$  ( $=\lambda$ ). If we substitute  $K[1 + \epsilon \sin(\omega\tau + \phi_0)]$  into  $K$  and expand  $f$  with respect to  $\epsilon K \sin(\omega\tau + \phi_0)$  to the first order, we obtain  $\lambda(\tau|\phi_0) = f(K, \nu) + [\partial f / \partial K(K, \nu)] \epsilon K \sin(\omega\tau + \phi_0)$ . Thus, we have

$$P(\tau|\phi_0) = \left[ f + \epsilon K \frac{\partial f}{\partial K} \sin(\omega\tau + \phi_0) \right] \times \exp \left[ -f\tau + \frac{\epsilon K}{\omega} \frac{\partial f}{\partial K} \{ \cos(\omega\tau + \phi_0) - \cos \phi_0 \} \right]. \quad (2)$$

We define  $\phi \in [0, 2\pi)$  as the phase of the modulating signal at the time when the next phase slip occurs. The phase  $\phi$  relates to  $\tau$  as  $\phi = \phi_0 + \omega\tau - 2\pi m$ , where  $m=1,2,\dots$  if  $\phi < \phi_0$  and  $m=0,1,\dots$  if  $\phi \geq \phi_0$ . If we change the variable  $\tau$  to  $\phi$  in Eq. (2), we can obtain the probability  $P_m(\phi|\phi_0)$  that the next phase slip occurs at  $\omega\tau = \phi - \phi_0 + 2\pi m$ . The probability that one phase slip occurs at  $\phi_0$  and the next one at  $\phi \in [0, 2\pi)$  is given by the sum of  $P_m$  over all possible  $m$  values:  $m=1,2,3,\dots$  for  $\phi < \phi_0$  and  $m=0,1,2,\dots$  for  $\phi \geq \phi_0$ . The explicit form of  $P(\phi|\phi_0)$  can be obtained from Eq. (2) as follows

$$P(\phi|\phi_0) = \begin{cases} F(\phi, \phi_0) e^{-\sigma} (1 - e^{-\sigma})^{-1}, & \phi < \phi_0, \\ F(\phi, \phi_0) (1 - e^{-\sigma})^{-1}, & \phi \geq \phi_0, \end{cases} \quad (3)$$

$$F(\phi, \phi_0) = \omega^{-1} \left( f + \epsilon K \frac{\partial f}{\partial K} \sin \phi \right) \times \exp \left[ -\frac{f}{\omega} (\phi - \phi_0) + \frac{\epsilon K}{\omega} \frac{\partial f}{\partial K} (\cos \phi - \cos \phi_0) \right], \quad (4)$$

where  $\sigma = 2\pi f/\omega$ .

Let  $W(\phi_0)$  be the probability distribution for the phase of the modulating signal at which a phase slip occurs. In the steady state,  $W$  has to satisfy the integral equation  $W(\phi_0) = \int_0^{2\pi} P(\phi_0|\phi')W(\phi')d\phi'$ , which leads to distribution  $W(\phi_0) = 1/(2\pi f)[f + \epsilon K(\partial f/\partial K)\sin\phi_0]$ . We can obtain the inter-slip interval distribution  $\rho(\tau)$  by integrating  $P(\tau|\phi_0)$  with the weight  $W(\phi_0)$  over  $\phi_0 \in [0, 2\pi)$ . The  $n$ th peak of  $\rho(\tau)$  is located at  $\tau_n = 2\pi n/\omega$ . Therefore, we can calculate the  $n$ th peak height as  $\rho(\tau_n) = [f + 1/(2f)]\{\epsilon K(\partial f/\partial K)\}^2 \exp(-f\tau_n)$ . With  $\epsilon=0$ , the value of  $\rho(\tau)$  at  $\tau = \tau_n$  is obtained as  $\rho_{\epsilon=0}(\tau_n) = f \exp(-f\tau_n)$  by setting  $\epsilon=0$ . If we subtract  $\rho_{\epsilon=0}(\tau_n)$  from  $\rho_{\epsilon \neq 0}(\tau_n)$ , then we obtain the difference  $\Delta\rho_n$  in the  $n$ th peak height between the two cases of  $\epsilon=0$  and  $\epsilon \neq 0$  as follows:

$$\Delta\rho_n(\nu) = \frac{1}{2f} \left( \epsilon K \frac{\partial f}{\partial K} \right)^2 \exp(-f\tau_n). \quad (5)$$

The difference  $\Delta\rho_n$  is a function of  $\nu$  since  $f$  and  $\partial f/\partial K$  depend on  $\nu$ . In Eq. (5),  $f$  and  $\partial f/\partial K$  are quantities that are defined in the signal free case ( $\epsilon=0$ ). This shows that whether or not  $\Delta\rho_n$  exhibits resonance behavior depends on the signal free properties of the system. Equation (5) indicates that  $\Delta\rho_n$  exhibits resonance behavior if  $f$  and  $(\partial f/\partial K)^2/f$  are increasing functions of  $\nu$ .

Next, we derive the functional form of  $f(K, \nu)$  from the dynamical properties of the system. The transition between the synchronization state with no phase slip and the desynchronization state with intermittent phase slips is shown to be caused by an unstable-unstable pair bifurcation crisis [6,10]. A stroboscopic map of system (1) is useful as regards observing this. A stroboscopic map  $\mathbf{M}: \mathbf{R}^3 \rightarrow \mathbf{R}^3$ ,  $(\Delta\theta_i, r_i, z_i) \mapsto (\Delta\theta_{i+1}, r_{i+1}, z_{i+1})$  can be defined by sampling the flow of system (1) at time  $t = 2\pi i/\Omega$ , where  $i$  is an integer.

It is shown in Ref. [6] that the attractor lies on a near two-dimensional manifold in  $(\Delta\theta, r, z)$  space, and  $\Delta\theta$  is defined on the line  $-\infty < \Delta\theta < \infty$ . When the system is in the synchronization state, there is an infinite array of such attractors spaced by  $2\pi$  in  $\Delta\theta$  because of the invariance of system (1) to the transformation  $\theta \mapsto \theta \pm 2\pi$ . There is no path that connects the different attractors.

When the system is in the desynchronization state, regions that were previously occupied by the different attractors, which we call the remnant attractors, are connected by certain trajectories. Here, the remnant attractor also lies on a near two-dimensional manifold. Figure 4 shows one of the remnant attractors, which is projected onto the  $(\Delta\theta, r)$  plane, along with blue points on the manifold that will move towards the next remnant attractor displaced from the presented one by  $2\pi$ . We call a set of these points a basin. The numerical method we used for depicting Fig. 4 is the same as that used in Ref. [6]. In Fig. 4, an example of a trajectory exhibiting a phase slip is also plotted by red  $\square$ . This trajectory moves from left to right passing through a narrow channel, which appears to be the only dominant channel in the parameter range we used. The motion through the channel is slow and similar to the period one motion. We show that this channel is created by a period one unstable-unstable pair

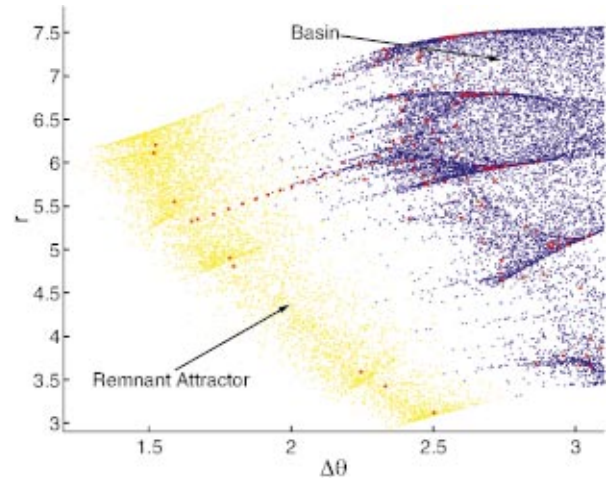


FIG. 4. (Color) Remnant attractor and basin. A trajectory exhibiting a phase slip is also plotted ( $\square$ ). Parameters are  $\epsilon=0$ ,  $K=0.07$ , and  $\nu=1.0032$ .

bifurcation crisis [11], whose process is as follows. There are two unstable fixed points on the attractor and the basin boundary of the next attractor when the parameters correspond to the synchronization state. As the parameters change, these fixed points approach each other, coalesce, and disappear. To demonstrate this process clearly, we define the displacement  $d_{min}$  of map  $\mathbf{M}$  as a function of  $\Delta\theta$  by  $d_{min} = \min_{r,z} \|\mathbf{M}(\Delta\theta, r, z) - (\Delta\theta, r, z)\|$ , where  $\mathbf{M}(\Delta\theta, r, z)$  stands for the image of a point  $(\Delta\theta, r, z)$  given by map  $\mathbf{M}$ . Figure 5 shows  $d_{min}$  plotted as a function of  $\Delta\theta$  for  $\nu=1.0038$  and some  $K$ s. By definition,  $d_{min}$  is zero at a fixed point. In Fig. 5, there are sharp decreases in  $d_{min}$  at two points for a large  $K$ , which correspond to the fixed points. These two fixed points approach each other, coalesce, and disappear as  $K$  decreases. This confirms the existence of the above-mentioned bifurcation process. In addition, the bifurcation point can be found at  $K_c = 0.1403$ .

We derive the form of  $f$  based on a theory proposed in Ref [10]. Near the bifurcation point, there are multipliers; one (approximately in the  $\Delta\theta$  direction, which we call the weakly unstable direction) is close to one and another (approximately in the  $r$  direction, which we call the strongly unstable direction) has an absolute value larger than one,

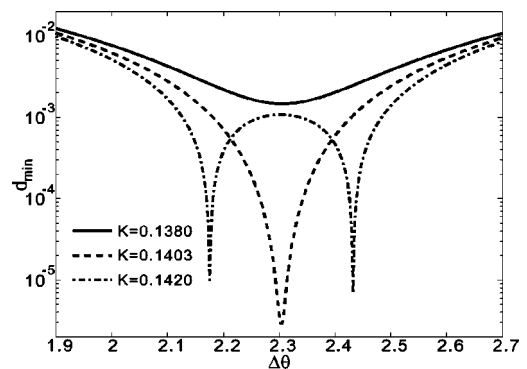


FIG. 5. Displacement  $d_{min}$  plotted against  $\Delta\theta$ . Parameters are  $\epsilon=0$  and  $\nu=1.0038$ .

which we denote by  $\mu$ . The other multiplier is disregarded since the motion is restricted to the manifold. The dynamics in the weakly unstable direction is the same as that for usual saddle-node bifurcation. Therefore, for any  $\nu$ , the time  $t_{sl}$  needed for the trajectory to pass through the channel can be scaled by  $t_{sl} \sim [K_c(\nu) - K]^{-1/2}$  [12]. An important point is that  $K_c$  is a function of  $\nu$ . If we expand  $K_c$  for  $\nu - \nu_0$ , we have  $t_{sl} \sim [K_c(\nu_0) + \{\partial K_c(\nu_0)/\partial \nu\}(\nu - \nu_0) - K]^{-1/2}$ . A trajectory can pass through the channel if the trajectory stays inside the channel for  $t_{sl}$ . The distance  $\Delta(t)$  from the channel center in the strongly unstable direction grows exponentially in time, i.e.,  $\Delta(t) \approx \Delta(0)|\mu|^t$ . Since  $\Delta(t)$  has to be smaller than the half width  $C'_1$  of the channel, we have  $\Delta(0) < C'_1 |\mu|^{-t_{sl}}$ . The trajectory initially has to visit a very small region on the remnant attractor to enter the channel, whose measure is proportional to  $C'_1 |\mu|^{-t_{sl}}$ . If we assume a uniform invariant probability density on the remnant attractor, the probability of the trajectory visiting the above small region during a unit time is also proportional to  $C'_1 |\mu|^{-t_{sl}}$ . This probability gives the slip rate  $f$ . Therefore, using the scaling law for  $t_{sl}$ , we arrive at

$$f \approx C_1 \exp \left[ -C_2 \left\{ K_c + \frac{\partial K_c}{\partial \nu} (\nu - \nu_0) - K \right\}^{-1/2} \right]. \quad (6)$$

In Fig. 6, we plot a numerical result of  $f(K, \nu)$  determined by the inverse of the average inter-slip interval  $\tau_{av}$  against  $[K_c(\nu) - K]^{-1/2}$  for certain values of  $\nu$ , where  $K_c(\nu)$  is determined from the  $d_{min}$  calculations. The theoretical result Eq. (6) is also shown by a dashed line in Fig. 6, where we

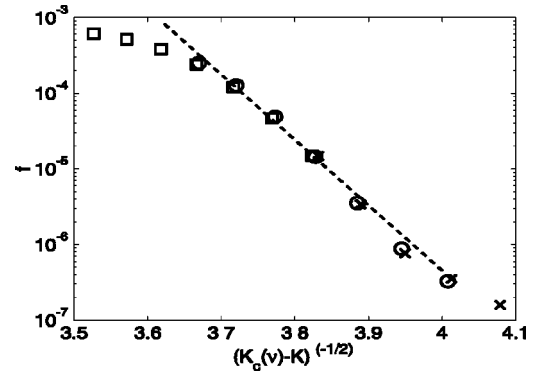


FIG. 6. Phase slip rate  $f$  plotted against  $[K_c(\nu) - K]^{-1/2}$ . Numerical results are shown for  $\nu = 1.0030$  ( $\times$ ),  $1.0036$  ( $\circ$ ), and  $1.0042$  ( $\square$ ). Scaling law Eq. (6) is also shown (dashed line).

determine  $\nu_0 = 1.0034$ ,  $K_c = 0.1362$ , and  $\partial K_c / \partial \nu = 10.25$  from the  $d_{min}$  calculations and  $C_1 = 1.62 \times 10^{28}$ , and  $C_2 = 19.89$  by least-square fitting to the numerical result of  $f$ . They agree with each other very well. We can readily find that for Eq. (6),  $f$  and  $(\partial f / \partial K)^2 / f$  are increasing functions of  $\nu$  in the parameter range we used. In Fig. 3, the theoretical curve of  $\Delta \rho_1$  obtained from Eqs. (5) and (6) actually shows resonant behavior and good agreement with the numerical curve. To conclude, the dynamical mechanism of DSR in system (1) can be explained by a two-parameter unstable-unstable pair bifurcation crisis. Since an unstable-unstable pair bifurcation crisis is one of typical crisis pattern, the present mechanism provides one of typical DSR mechanism. Furthermore, it is expected that this approach to explanation of DSR can widely be applied to other types of crises.

- [1] L. Gammaitoni, P. Hänggi, P. Jung, and F. Marchesoni, *Rev. Mod. Phys.* **70**, 223 (1998).
- [2] V.S. Anishchenko, A.B. Neiman, and M.A. Safanova, *J. Stat. Phys.* **70**, 183 (1993).
- [3] M. Franaszek and E. Simiu, *Phys. Rev. E* **54**, 1298 (1996).
- [4] E. Reibold, W. Just, J. Becker, and H. Benner, *Phys. Rev. Lett.* **78**, 3101 (1997).
- [5] A.N. Pisarchik and R. Corbalán, *Phys. Rev. E* **58**, R2697 (1998).
- [6] E. Rosa, Jr., E. Ott, and M.H. Hess, *Phys. Rev. Lett.* **80**, 1642 (1998).
- [7] M.G. Rosenblum, A.S. Pikovsky, and J. Kurths, *Phys. Rev.*

*Lett.* **76**, 1804 (1996).

- [8] K. Wiesenfeld, D. Pierson, E. Pantazelou, C. Dames, and F. Moss, *Phys. Rev. Lett.* **72**, 2125 (1994).
- [9] M.H. Choi, R.F. Fox, and P. Jung, *Phys. Rev. E* **57**, 6335 (1998).
- [10] A. Pikovsky, G. Osipov, M. Rosenblum, M. Zaks, and J. Kurths, *Phys. Rev. Lett.* **79**, 47 (1997).
- [11] C. Grebogi, E. Ott, and J.A. Yorke, *Phys. Rev. Lett.* **50**, 935 (1983).
- [12] E. Ott, *Chaos in Dynamical Systems* (University Press, Cambridge, 1993).